

7-9-2014

Effective cluster typical medium theory for the diagonal Anderson disorder model in one- and two-dimensions

Chinedu E. Ekuma
Louisiana State University

Hanna Terletska
Louisiana State University

Zi Yang Meng
Louisiana State University

Juana Moreno
Louisiana State University

Mark Jarrell
Louisiana State University

See next page for additional authors

Follow this and additional works at: https://digitalcommons.lsu.edu/physics_astronomy_pubs

Recommended Citation

Ekuma, C., Terletska, H., Meng, Z., Moreno, J., Jarrell, M., Mahmoudian, S., & Dobrosavljević, V. (2014). Effective cluster typical medium theory for the diagonal Anderson disorder model in one- and two-dimensions. *Journal of Physics Condensed Matter*, 26 (27) <https://doi.org/10.1088/0953-8984/26/27/274209>

This Article is brought to you for free and open access by the Department of Physics & Astronomy at LSU Digital Commons. It has been accepted for inclusion in Faculty Publications by an authorized administrator of LSU Digital Commons. For more information, please contact ir@lsu.edu.

Authors

Chinedu E. Ekuma, Hanna Terletska, Zi Yang Meng, Juana Moreno, Mark Jarrell, Samiyeh Mahmoudian, and Vladimir Dobrosavljević

Effective Cluster Typical Medium Theory for Diagonal Anderson Disorder Model in One- and Two-Dimensions

Chinedu E. Ekuma,^{1,2,*} Hanna Terletska,^{1,3} Zi Yang Meng,^{1,2} Juana Moreno,^{1,2}
Mark Jarrell,^{1,2,†} Samiyeh Mahmoudian,⁴ and Vladimir Dobrosavljević⁴

¹*Department of Physics & Astronomy Louisiana State University, Baton Rouge, LA 70803, USA*

²*Center for Computation and Technology, Louisiana State University, Baton Rouge, LA 70803, USA*

³*Brookhaven National Laboratory, Upton, New York 11973, USA*

⁴*Department of Physics, Florida State University, Tallahassee, FL 32301, USA*

(Dated: June 23, 2014)

We develop a cluster typical medium theory to study localization in disordered electronic systems. Our formalism is able to incorporate non-local correlations beyond the local typical medium theory in a systematic way. The cluster typical medium theory utilizes the momentum resolved typical density of states and hybridization function to characterize the localization transition. We apply the formalism to the Anderson model of localization in one- and two-dimensions. In one dimension, we find that the critical disorder strength scales inversely with the linear cluster size with a power-law, $W_c \sim (1/L_c)^{1/\nu}$; whereas in two dimensions, the critical disorder strength decreases logarithmically with the linear cluster size. Our results are consistent with previous numerical work and in agreement with the one-parameter scaling theory.

PACS numbers: 71.23.An,71.23.-k,72.15.Rn,71.23.-k, 71.55.Jv,05.60.Gg

Keywords: CTMT, Anderson localization, Typical density of states, Hybridization rate

I. INTRODUCTION

Over the past several decades, disorder-driven (Anderson) localization has been a subject of intensive theoretical^{1–13} and experimental^{14–21} studies. It has recently been realized experimentally with atomic matter waves.^{22–24} In the original seminal paper of Anderson,³ localization is defined as the absence of diffusion. It generally arises from quantum interference between different particle trajectories and depends strongly on the dimensionality of the system. According to the one-parameter scaling theory,¹ there is no delocalized phase in one- and two- dimensions, whereas, a metal-insulator-transition (localization/delocalization phase) occurs at finite disorder strength in three-dimensions (3D). Effective medium theories like the coherent potential approximation (CPA)¹⁰ and its cluster extensions, including the dynamical cluster approximation (DCA),^{25–27} average over disorder, favoring a metallic solution, and fail to capture the localized state in 1 and 2D, and even the transition in 3D.

Here, we develop an extension of the Typical Medium Theory⁹ which is able to capture the localized state. The study of disordered systems rely on probability distribution functions (PDFs) to measure ‘random’ quantities of interest. To characterize localization, the most important quantity in the majority of physical or statistical problems is usually the “typical” value of the ‘random’ variable, which corresponds to the most probable value of the PDF.²⁸ In most systems the nature of the PDF is not known a priori; as such, we have limited information via the moments or cumulants of the PDFs. Under such situation, the “typical” or the most probable value of the PDF²⁸ contains important and direct information. Different from some systems where the first moment (the

arithmetic average) is a good estimate of the random variable, the Anderson localization is a non-self-averaging phenomenon. Close to the critical point the electronic quantities fluctuate strongly and the corresponding PDF of the local density of states is very asymmetric with long tails^{29,30} such that infinitely many moments are needed to describe it.²⁸ In some cases, the corresponding moments might not even exist especially close to the critical point.³¹

The arithmetic average of random one-particle quantities is not critical at the Anderson localization transition. This is the reason that most mean field theories like the CPA¹⁰ and its cluster extensions including the DCA,^{25–27} fail to provide a proper description of Anderson localization in disordered systems. This failure is intrinsic to these theories as the algebraically averaged quantities, i.e., averaged density of states, used in these methods always favor the metallic state. This can be understood from the fact that in an infinite system with localized states, the average density of states will remain continuous while the local density of states become discrete. See for e.g., Refs. 4,9,29,32–35 for a detailed discussion.

In contrast to the arithmetic average, the geometrical average,^{9,29,30,34,36} gives a better approximation to the most probable value of the local density of states. Dobrosavljević et al.⁹ proposed the typical medium theory (TMT) to study disorder system, where the arithmetically averaged local density of states is replaced with the typical density of states (TDOS), where the geometrical average is used. They demonstrated that the TDOS vanishes continuously as the disorder strength increases towards the critical point, and it can be used as an effective mean field order parameter for the Anderson localization.

However, the TMT proposed in Ref. 9 is a single-site self-consistent mean field theory. Due to its local nature,

it fails to capture the effect of spatial correlations. In this work, we extend the local typical medium theory⁹ to a cluster version utilizing the ideas from the dynamical cluster approximation.^{25–27} The DCA systematically incorporates spatial inter-site correlations. Therefore quantum coherence, which is important for Anderson localization, is captured. This is the key motivation of our work. A concomitant motivation is that recent theoretical work shows that rare events¹² play an important role in Anderson localization; our formalism might be able to take rare events into consideration.

We develop a cluster typical medium theory (CTMT) for studying disorder systems. Our cluster self-consistent mean field theory systematically incorporates non-local correlation effects into the local TMT (for a review of cluster approximation see Refs. 26,37). In our formalism, the typical density of states (TDOS) is calculated using the geometrical average of the imaginary part of the Green function. We utilize the TDOS and the hybridization rate to characterize the localization transition. The imaginary part of the hybridization rate measures the hopping amplitude or diffusion of electrons from the cluster to the typical medium (c.f. Fig. 1 (a)). Then, the point where this quantity vanishes corresponds to the absence of diffusion and the onset of Anderson localization. We also note that the TDOS vanishes at the same point as the hybridization rate. We apply the developed CTMT approach to study the non-interacting Anderson model in one and two dimensions, and we briefly describe the failure of the method in three dimensions. For a review of the progress in lower dimensional Anderson localization, see for e.g., Refs. 5,16,38–42. Our results show that the CTMT provides a proper mean field description of Anderson localization for lower dimensional systems. While the present study is for diagonal Anderson disorder model, the method can easily be extended to other disorder distributions like Gaussian, binary disorder, etc.

The rest of this paper is organized as follows. After Section I, the basic formalism and description of the CTMT self-consistency is provided in Section II. Section III shows our computed results. We conclude in Section IV.

II. MODEL AND FORMALISM

We consider the Anderson model³ with a diagonal on-site random disorder potential. The Hamiltonian is given by

$$\hat{H} = -t \sum_{\langle i,j \rangle} (c_i^\dagger c_j + c_j^\dagger c_i) + \sum_i (V_i - \mu) n_i. \quad (1)$$

The operators $c_i^\dagger(c_i)$ create (annihilate) a quasi-particle in a Wannier orbital on site i and $n_i = c_i^\dagger c_i$ is the number operator, μ is the chemical potential, and t is the hopping matrix element between nearest-neighbor $\langle i, j \rangle$, which we set $4t = 1$ as the energy unit. The local potentials

$V_i \in [-W, +W]$ are randomly distributed according to a probability distribution $P(V_i)$ with a box distribution function:

$$P(V_i) = \frac{1}{2W} \Theta(W - |V_i|) \quad (2)$$

where the strength of the disorder in units of $4t$ is parametrized by the width W of the box, and $\Theta(x)$ is the step function.

The cluster typical medium theory (CTMT) combines the self-consistent frameworks of the DCA²⁵ and the single site TMT approaches.⁹ In particular, the CTMT maps the given disordered lattice system into a finite cluster which is embedded in an effective self-consistent typical medium (c.f. Fig. 1(a)). Note that unlike in the usual DCA scheme where the effective medium is constructed via algebraic averaging over disorder configurations, in the CTMT scheme, geometric averaging is used. By mapping a d -dimensional lattice containing N sites to a finite

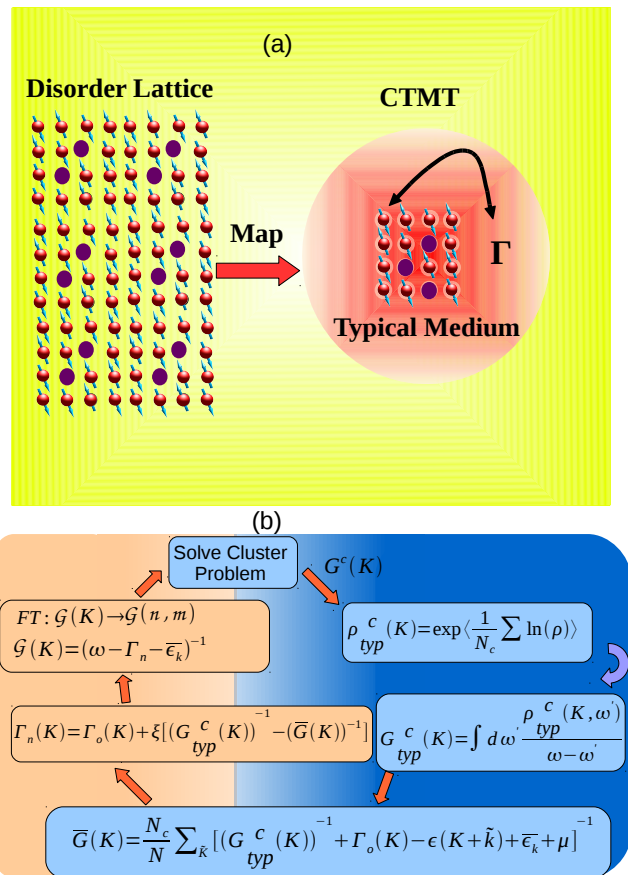


FIG. 1: (Color online) (a) A schematic one-dimensional diagram of the environment of the cluster typical medium theory (CTMT). This diagram depicts the mapping of a disordered, infinite lattice to a finite cluster self-consistently embedded in the typical effective medium. (b) The self-consistent loop of the computational procedure of the cluster typical medium theory.

small cluster containing $N_c = L_c^d$ sites, where L_c is the linear dimension of the cluster, we dramatically reduce the computation effort.²⁶ Unlike the single-site methods commonly used to study disordered systems, such as the coherent potential approximation (CPA)^{10,43} or the local TMT,⁹ the CTMT ensures that non-local, spatial fluctuations, which are neglected in single-site approaches, are systematically incorporated as the cluster size N_c increases. Short length scale correlations inside the cluster are treated with exact numerical methods such as Monte Carlo (MD) or exact diagonalization, while long length scale correlations are treated within the typical medium (c.f. Fig. 1(a)). At the limit of cluster size $N_c = 1$, the CTMT recovers the local TMT, and at the limit of $N_c \rightarrow \infty$, the CTMT becomes exact. Hence, between these two limits, the CTMT systematically incorporates non-local correlations into the local TMT.

Let us describe our formalism in detail. In the DCA, the average density of states (DOS) at each cluster momentum K is defined as

$$\rho_{avg}^c(K, \omega) = \langle \rho^c(K, \omega) \rangle = -\frac{1}{\pi} \langle \text{Im} G^c(K, K, \omega) \rangle, \quad (3)$$

where the superscript ‘ c ’ denotes cluster, and $\langle \rangle$ is the disorder average. For a single site $N_c = 1$, we recover the CPA. The K -dependent cluster Green function is obtained from the site dependent Green function $G_c(i, j, \omega)$ via

$$G^c(K, K, \omega) = \frac{1}{N_c} \sum_{i,j} e^{iK \cdot (R_i - R_j)} G_c(i, j, \omega). \quad (4)$$

In the CTMT, we first obtain $\rho^c(K, \omega) = -\text{Im} G^c(K, K, \omega)/\pi$ for each cluster disorder configuration. It is easy to show, using the Lehmann representation,^{44,45} that $\rho^c(K, \omega) \geq 0$ for each K, ω , and disorder configuration. We then calculate using geometric averaging the cluster-momentum-resolved typical density of states (TDOS) for each K as

$$\rho_{typ}^c(K, \omega) = \exp \langle \ln \rho^c(K, \omega) \rangle. \quad (5)$$

To ensure the causality of the Green function, we carry out the Hilbert transformation of the TDOS to obtain the typical cluster Green function as

$$G_{typ}^c(K, \omega) = \int d\omega' \frac{\rho_{typ}^c(K, \omega')}{\omega - \omega'}. \quad (6)$$

And we use the typical Green function to continue the self-consistency loop. A schematic diagram of the CTMT self-consistency loop is shown in Fig. 1(b). We have adopted the hybridization rate function $\Gamma(K, \omega)$ as the order parameter to control the convergence. This stems from the fact that $\text{Im}(\Gamma(K, \omega))$ measures the rate of electron hybridization between the cluster and the typical medium. When $\text{Im}(\Gamma(K, \omega))$ is zero, the hopping between cluster and medium vanishes and the electrons in

the system are localized. We note that at this point the TDOS also becomes zero, as such, the TDOS and $\text{Im}(\Gamma(K, \omega))$ act as mean field order parameters within our effective medium for detecting Anderson localization. The CTMT iterative procedure is described as follows:

1. We start by proposing an initial hybridization function $\Gamma_o(K, \omega)$, where the subscript o denotes old. The choice of the starting guess for the hybridization function may be based on a priori knowledge, i.e., in case we have information about the self-energy $\Sigma(K, \omega)$ and cluster Green function $G^c(K, \omega)$, $\Gamma_o(K, \omega)$ can be calculated as

$$\Gamma_o(K, \omega) = \omega - \bar{\epsilon}(K) - \Sigma(K, \omega) - 1/G^c(K, \omega) \quad (7)$$

where $\bar{\epsilon}(K) = \frac{N_c}{N} \sum_{\tilde{k}} \epsilon(K + \tilde{k})$ is the coarse-

grained bare dispersion with \tilde{k} summed over N/N_c momenta inside the cell centered at the cluster momentum K .²⁷ However, if nothing is known a priori, the guess $\Gamma_o(K, \omega) \equiv 0$ may serve as the starting point.

2. The cluster problem is now set-up by calculating the cluster-excluded Green function $\mathcal{G}(K, \omega)$ as

$$\mathcal{G}(K, \omega) = (\omega - \Gamma_o(K, \omega) - \bar{\epsilon}(K))^{-1}. \quad (8)$$

Since the cluster problem is solved in real space, we then Fourier transform $\mathcal{G}(K, \omega)$: $\mathcal{G}_{n,m} = \sum_K \mathcal{G}(K) \exp(iK \cdot (r_n - r_m))$.

3. Next, we solve the cluster problem using, e.g., a MC simulation. Here, we stochastically generate random configurations of the disorder potential V . For each disordered configuration, we use the Dyson equation to calculate the new fully dressed cluster Green function

$$G^c(V) = (\mathcal{G}^{-1} - V)^{-1}. \quad (9)$$

This is Fourier transformed to $G^c(K, K, \omega)$ to obtain the cluster density of states $\rho^c(K, \omega) = -\frac{1}{\pi} \text{Im} G^c(K, K, \omega)$. The typical cluster density of states is then calculated via geometric averaging using Eq. 5. Then, we calculate the disorder averaged, typical cluster Green function $G_{typ}^c(K, \omega)$ via Hilbert transform using Eq. 6.

4. With the cluster problem solved, we use the typical cluster Green function $G_{typ}^c(K, \omega)$, to calculate the coarse-grained cluster Green function $\bar{G}(K, \omega)$ as

$$\bar{G}(K, \omega) = \frac{N_c}{N} \sum_{\vec{k}} \frac{1}{(G_{typ}^c(K, \omega))^{-1} + \Gamma_o(K, \omega) - \epsilon(K + \vec{k}) + \bar{\epsilon}(K) + \mu}. \quad (10)$$

5. Finally, we calculate the new hybridization function using linear mixing

$$\Gamma_n(K, \omega) = \Gamma_o(K, \omega) + \xi[(G_{typ}^c(K, \omega))^{-1} - (\bar{G}(K, \omega))^{-1}] \quad (11)$$

where the subscripts n and o denote new and old, respectively. The mixing parameter $\xi > 0$ controls the ratio of the new and old $\Gamma(K, \omega)$ entering the next iteration. For very small ξ , convergence may be slowed down unnecessarily, while for very large ξ , oscillations about the self-consistent solution may occur. Instead of linear mixing, the convergence of the computations can be improved by using the Broyden method⁴⁶.

6. We repeat this procedure until the hybridization function converges to the desired accuracy, $\Gamma_o(K, \omega) = \Gamma_n(K, \omega)$. When this happens, the Green functions are also converged, $\bar{G}(K, \omega) = G_{typ}^c(K, \omega)$ within the computational error.

We note that instead of using the hybridization function $\Gamma(K, \omega)$ in the self-consistency, one can also use the self-energy $\Sigma(K, \omega)$. Both procedures should lead to the same solution since they are related by Eq. 7.

This method is causal, provided that the cluster solver produces a causal result. The argument is the same as that for the DCA²⁷ and will not be repeated here.

III. RESULTS AND DISCUSSION

We apply the CTMT scheme to one- and two-dimensional disordered systems describe by the Hamiltonian in Eq. 1. Fig. 2 shows the local typical density of states (TDOS($R=0$)) for a cluster of size $N_c = 8$ at various disorder strengths. For both one- and two-dimensional systems, the TDOS systematically goes to zero as the disorder strength is gradually increased. In 1D, the TDOS is practically zero for all frequencies at a critical disorder strength $W_c \approx 0.8$; whereas in 2D, $W_c \approx 2.3$. Above the critical disorder strength, the electrons are localized. The TDOS calculated in our CTMT scheme indeed provides key information about the Anderson localization transition.

According to the one-parameter scaling theory,^{1-3,5} in 1D an arbitrary weak disorder strength localizes the electrons; whereas in 2D, the system is also always localized, but with the difference that the conductivity only decreases logarithmically with disorder strength.

As we discussed in preceding sections, mean field theories, such as the single-site CPA, or the DCA, cannot capture the localization transition due to the use of an algebraic averaging scheme in their self-consistency. The single-site TMT, on the other hand, is able to qualitatively describe the localization transition in one, two and three dimensions,¹¹ but with critical disorder strength different from the exact values, i.e., in 1D and 2D, $W_c = 0$ and in 3D $W_c = 2.1$ (in units where $4t = 1$).^{6,9,11} This is not surprising as the local TMT completely neglects non-local inter-site correlations. The CTMT proposed in this paper gives a better qualitative and quantitative mean field theory for studying disordered systems in one and two-dimensions. We expect that as the cluster sizes increases, the critical disorder strength will systematically converge to the exact value of zero in the thermodynamic limit. This is demonstrated in Figs. 3 and 4.

Figure 3 shows the local typical density of states at the band center, TDOS($R = 0, \omega = 0$), for a one-dimensional system as a function of disorder strength, W . By increasing the cluster size the critical disorder strength decreases and eventually will go to zero for a reasonably large N_c . Similarly, Fig. 4 displays the local typical density of states at the band center for a two-dimensional system. The

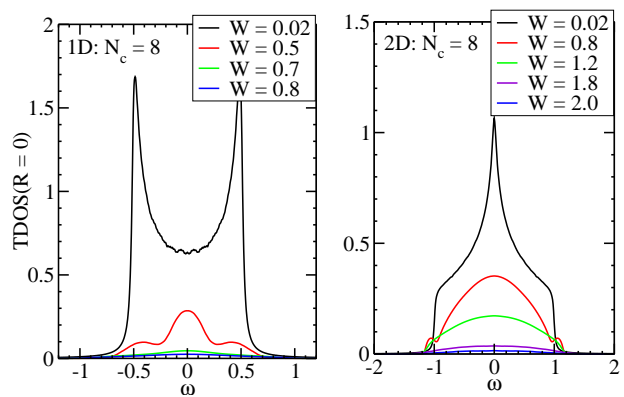


FIG. 2: (Color online) The local typical density of states, TDOS($R=0$), as a function of frequency for various disorder strengths, W , for clusters of size $N_c = 8$ for one- (left panel) and two- (right panel) dimensional systems. Observe that in both cases, the TDOS gradually decreases with increasing W . The value of W where the TDOS vanishes reveals the critical disorder strength W_c . Hence the TDOS behaves as an order parameter for the localization transition. $\text{Im } \Gamma(R = 0, \omega)$ (not shown) vanishes at the same critical disorder strength as the TDOS.

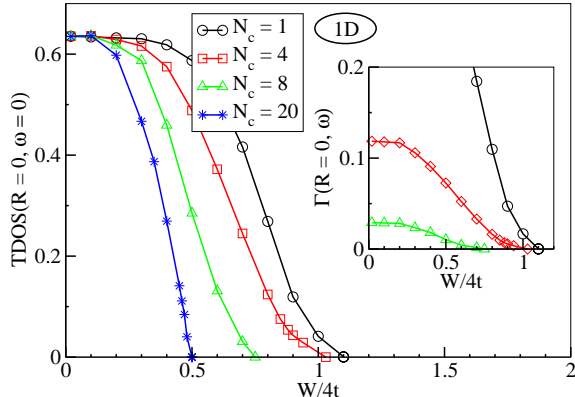


FIG. 3: (Color online) The local typical density of states at the band center, $\text{TDOS}(R=0, \omega=0)$, for one-dimension as a function of the disorder strength, $W/4t$, for various cluster sizes. The critical disorder strength W_c decreases as the cluster size N_c increases. The inset displays the local hybridization rate at the band center $\Gamma(R=0, \omega=0)$ vs. $W/4t$. Note that $\Gamma(R=0, \omega=0)$ and $\text{TDOS}(R=0, \omega=0)$ go to zero at the same critical disorder strength.

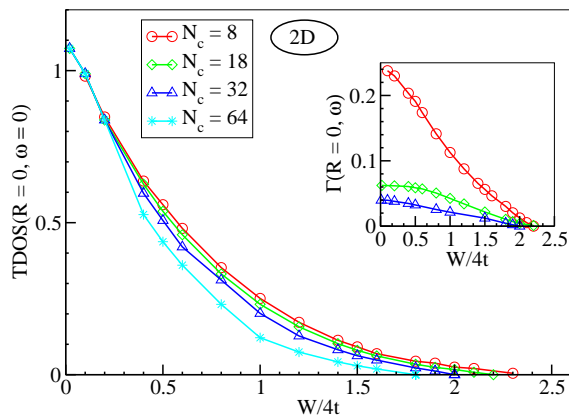


FIG. 4: (Color online) The local typical density of states at the band center, $\text{TDOS}(R=0, \omega=0)$, for a two-dimensional system as a function of disorder strength, $W/4t$, for various cluster sizes. The critical disorder strength W_c decreases as cluster size N_c increases.

critical disorder strength also decreases as N_c increase. However, the decrease of W_c as a function of N_c is slower than that of the 1D case. This implies that the scaling form of W_c vs N_c (or L_c) for 1D and 2D systems is different. The former follows a power-law whereas the latter has a logarithmic form. This is consistent with the

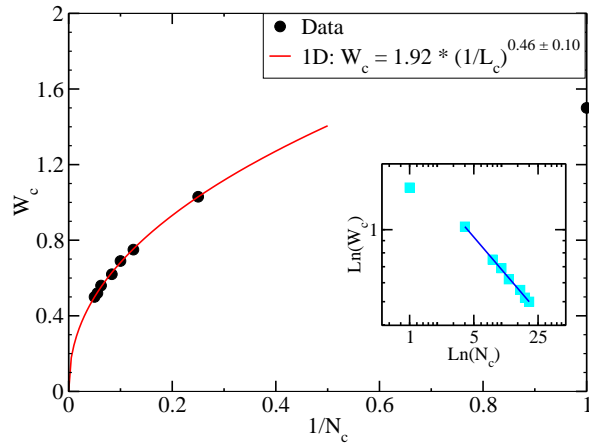


FIG. 5: (Color online) The critical disorder strengths W_c for various cluster sizes $N_c (= L_c)$ in a 1D disordered system. The data can be fitted with a scaling ansatz: $\xi = L_c \sim W_c^{-\nu}$ or $W_c \sim (1/L_c)^{1/\nu}$, with $1/\nu = 0.46 \pm 0.10$ in agreement with previous numerical results of $1/\nu = 0.5^{47}$. The inset shows the power law behavior in a log-log plot.

one-parameter scaling theory^{1-3,5} which shows that a 1D system is strongly localized, while 2D is the lower critical dimension of the Anderson localization transition. The insets of Figs. 3 and 4 show that the local hybridization rate at the band center, $\Gamma(R=0, \omega=0)$, goes to zero at the same value of W than the TDOS.

Figs. 5 and 6 address the scaling of W_c vs N_c . In 1D, the scaling ansatz is $\xi = L_c \sim W_c^{-\nu}$, where ξ is the localization length, and ν the critical exponent. As shown in Fig. 5, the power law behavior is nicely captured by our data with $1/\nu = 0.46 \pm 0.10$ in basic agreement with previous numerical results which reported a value of $1/\nu = 0.5$,⁴⁷ and also with the one-parameter scaling theory.¹ The inset of Fig. 5 is a log-log plot of W_c vs N_c where the power-law behavior $W_c \sim (1/L_c)^{1/\nu}$ is seen as a straight line.

Figure 6 displays the scaling of W_c vs L_c ($N_c = L_c^2$) in a 2D system. Our data can be fit with a logarithmic function, $W_c = 695.97/(179.91 + 96.8 \times \ln(L_c))$. Therefore, the critical disorder strength decreases slowly with cluster size and only for very large clusters the system is completely localized. This behavior agrees with the one-parameter scaling theory,¹ as 2D is generally believed to be the lower critical dimension for the Anderson localization.⁴⁸ The inset of Fig. 6 is a semi-log plot of W_c vs $\ln N_c$ where the logarithmic behavior is seen as a straight line. We note that our data fit nicely to an exponent form: $L_c = \exp(4.73/V_c^{0.98})/V_c^{0.98}$ in basic agreement with the results of MacKinnon and Kramer².

The present study clearly presents the essence of the effective typical medium theory, and the need to systematically go beyond single site approximations. Our formalism can easily be extended to study other physical

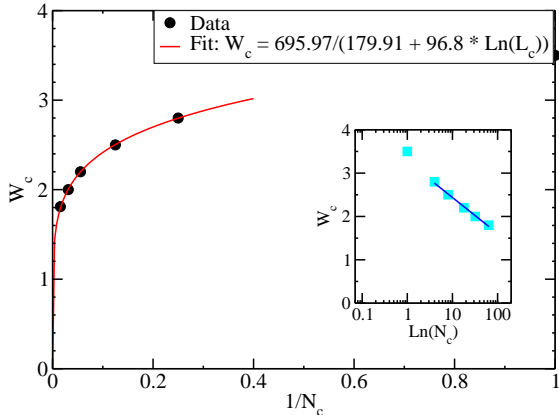


FIG. 6: (Color online) The critical disorder strength W_c for various cluster sizes $N_c = L_c^2$ in a 2D disordered system. The data can be fit with a scaling ansatz: $W_c = 695.97/(179.91 + 96.8 \times \ln(L_c))$ in agreement with the results of MacKinnon and Kramer². The inset shows the logarithmic behavior in a semi-log plot.

phenomenon in lower dimensions. For example, in 1D systems, one can easily extend this approach to study super diffusion,⁴⁹ which may not be possible in the local TMT approach, since the resonant states leading to super diffusion are non-local. This present formalism can also be extended to study off-diagonal disorder in delocalization/localization processes in low dimensions.^{50–52}

As explained in the previous sections, when system becomes localized, the PDFs of the density of states change from Gaussian distribution (where all states are metallic, the PDF is symmetric with the shape of TDOS the same as the ADOS) to a very asymmetric distribution with long tails (where all states are localized, the LDOS strongly fluctuating at all sites, and the TDOS is very different from the ADOS). Utilizing large-scale exact diagonalization calculations, Schubert *et al.*⁷ have demonstrated that the PDFs close to the Anderson transition in 2D and 3D systems are log-normal. Here, as a proof of principle, we perform similar calculations. Within the CTMT scheme, we obtain the PDFs of the momentum-resolved DOS $\rho(K, \omega = \bar{\epsilon}_K)$ at different momenta cells centered at cluster momentum point K and at the averaged energy $\omega = \bar{\epsilon}_K$ of the cell K . When sampled over large enough number of disorder configurations in our MC procedure, we indeed find as the disorder strength W is increasing, the PDF $[\rho(K, \omega = \bar{\epsilon}_K)]$ (shown in Figs. 7 and 8 for 1D and 2D systems, respectively) develop log-normal distributions, consistent with the observation in Ref. 7. Moreover, we find for 1D system, the log-normal distribution happens for all the momentum cells at a very small disorder strength ($W = 0.4, 0.5$) for $N_c = 8$ cluster; and in 2D, the same log-normal distribution for all

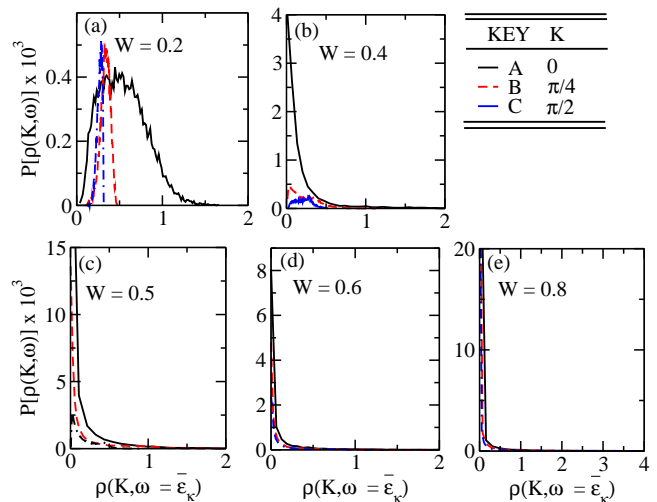


FIG. 7: (Color Online). The evolution of the probability distribution (PDF $[\rho(K, \omega = \bar{\epsilon}_K)]$) at different cluster cells with increasing W for 1D system, the cluster size is $N_c = 8$. The labels A–C correspond to three cluster momenta. At very small disorder strength $W \approx 0.4, 0.5$, (cf. Fig. 7(b),(c)), all the cells show log-normal distribution.

the cells will only happen at a larger disorder strength ($W = 1.0, 1.2$). This observation is consistent with the fact that 1D systems is much easier to localize as compared to 2D systems.

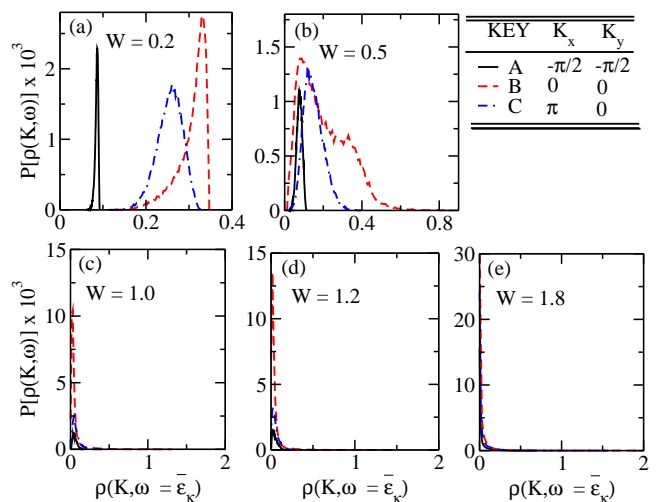


FIG. 8: (Color Online). The evolution of the probability distribution (PDF $[\rho(K, \omega = \bar{\epsilon}_K)]$) at different cluster cells with increasing W for 2D system, the cluster size is $N_c = 8$. The labels A–C correspond to three cluster momenta. At small disorder strength, the PDF of some cells still remain Gaussian (cf. Fig. 7(a)-(b)). While as the disorder strength increases, (cf. Fig. 7(c),(d)), all the cells show log-normal distribution.

We also applied this approach to study three-dimensional systems. Unfortunately, our formalism, when applied with modest cluster sizes, is unable to fully

capture the localization transition in 3D. First, we observe an unsystematic behavior of our formalism in the sense that for small cluster size, for e.g., $N_c=1, 4$ and 8 , the critical disorder strength W_c , where all states become localized, is underestimated, while for larger cluster sizes, e.g., $N_c=24$ and 38 , it overestimates the critical disorder strength. Of course, in the limit of large N_c , the CTMT recovers the exact critical behavior around W_c . Second, for modest cluster sizes, while the TDOS becomes small as W increases, its width increases monotonically with disorder strength until the critical value is reached. However, in exact diagonalization calculations the width first increases and then decreases with disorder strength,^{11,53,54} indicating that our current formalism fails to correctly capture the localization edge for modest cluster sizes. In addition, while the hybridization rates also become small, they do not all vanish at the critical disorder strength W_c . Rather, only the hybridizations corresponding to states near the top and bottom of the bands vanish while the states at the band center only vanish for values of the disorder strength much larger than W_c . Apparently, while our current CTMT formalism is able to capture weak localization effects in lower dimensional systems, it is not able to capture the evolution of the localization edge which characterizes the transition in three dimensions until the cluster sizes are very large. We are working to develop a fully causal for-

malism which is able to efficiently capture the localization transition in 3D.

IV. CONCLUSION

We develop a cluster extension to the local typical medium theory via the dynamical cluster approximation for studying localization in low dimensional disordered electronic systems. The developed CTMT systematically incorporates nonlocal corrections to capture quantum coherence. The formalism recovers the local TMT when the cluster size is $N_c = 1$, and becomes exact as $N_c \rightarrow \infty$. Such an approach opens a new avenue to study localization effects in lower dimensional model systems.

Acknowledgments. We thank K. M. Tam and S. X. Yang for useful discussions. Work at LSU is funded by the National Science Foundation LA-SIGMA award: EPS-1003897. Work at BNL is supported by the U.S. Department of Energy (DOE) under contract DE-AC02-98CH10886. High performance computational resources are provided by Louisiana Optical Network Initiative (LONI), and HPC@LSU computing resources. Work at FSU is supported by the National High Magnetic Field Laboratory and the NSF Grant No. DMR-1005751.

-
- * Electronic Address: cekuma1@lsu.edu
† Electronic Address: jarrellphysics@gmail.com
- ¹ E. Abrahams, P. W. Anderson, D. C. Licciardello, and T. V. Ramakrishnan, Phys. Rev. Lett. **42**, 673 (1979).
 - ² A. MacKinnon and B. Kramer, Phys. Rev. Lett. **47**, 1546 (1981).
 - ³ P. W. Anderson, Phys. Rev. **109**, 1492 (1958).
 - ⁴ A. Lagendijk, B. van Tiggelen, and D. S. Wiersma, Physics Today **62**, 24 (2009).
 - ⁵ P. A. Lee and T. V. Ramakrishnan, Rev. Mod. Phys. **57**, 287 (1985).
 - ⁶ K. Slevin and T. Ohtsuki, Phys. Rev. Lett. **82**, 382 (1999).
 - ⁷ G. Schubert, J. Schleede, K. Byczuk, H. Fehske, and D. Vollhardt, Phys. Rev. B **81**, 155106 (2010).
 - ⁸ J. P. Pichard and G. Sarma, J. Phys. C **14**, L127 (1981).
 - ⁹ V. Dobrosavljević, A. A. Pastor, and B. K. Nikolić, Europhysics Letters **62**, 76 (2003).
 - ¹⁰ R. J. Elliott, J. A. Krumhansl, and P. L. Leath, Rev. Mod. Phys. **46**, 465 (1974).
 - ¹¹ Y. Song, W. A. Atkinson, and R. Wortis, Phys. Rev. B **76**, 045105 (2007).
 - ¹² R. N. Bhatt and S. Johri, Int. J. Mod. Phys.: Conf. Ser. **11**, 79 (2012).
 - ¹³ L. P. Gorkov, A. I. Larkin, and D. E. Khmel'nitskii, Sov. Phys. JETP Lett. **30**, 228 (1979).
 - ¹⁴ A. H. Clark, Phys. Rev. **154**, 750 (1967).
 - ¹⁵ M. Morgan and P. A. Walley, Philos. Mag. **23**, 661 (1971).
 - ¹⁶ B. Kramer and A. MacKinnon, Reports on Progress in Physics **56**, 1469 (1993).
 - ¹⁷ D. Y. Sharvin and Y. V. Sharvin, Sov. Phys. JETP Lett. **34**, 272 (1982).
 - ¹⁸ G. Bergmann, Phys. Rep. **107**, 1 (1984).
 - ¹⁹ S. V. Kravchenko, G. V. Kravchenko, J. E. Furneaux, V. M. Pudalov, and M. D'Iorio, Phys. Rev. B **50**, 8039 (1994).
 - ²⁰ S. V. Kravchenko and M. P. Sarachik, Rep. Prog. Phys. **67**, 1 (2004).
 - ²¹ E. Abrahams, S. V. Kravchenko, and M. P. Sarachik, Rev. Mod. Phys. **73**, 251 (2001).
 - ²² J. Billy, V. Josse, Z. Zuo, A. Bernard, B. Hambrecht, P. Lugan, D. Clement, L. Sanchez-Palencia, P. Bouyer, and A. Aspect, Nature **453**, 891 (2008).
 - ²³ G. Roati, C. D'Errico, L. Fallani, M. Fattori, C. Fort, M. Zaccanti, G. Modugno, M. Modugno, and M. Inguscio, Nature **453**, 895 (2008).
 - ²⁴ J. Chabé, G. Lemarié, B. Grémaud, D. Delande, P. Szriftgiser, and J. C. Garreau, Phys. Rev. Lett. **101**, 255702 (2008).
 - ²⁵ M. Jarrell and H. R. Krishnamurthy, Phys. Rev. B **63**, 125102 (2001).
 - ²⁶ T. Maier, M. Jarrell, T. Pruschke, and M. H. Hettler, Rev. Mod. Phys. **77**, 1027 (2005).
 - ²⁷ M. H. Hettler, M. Mukherjee, M. Jarrell, and H. R. Krishnamurthy, Phys. Rev. B **61**, 12739 (2000).
 - ²⁸ The most probable value of a random quantity is the mode, which is the value for which its PDF becomes maximal. A property X of a given system is self-averaging if 'most' realizations of the randomness in the thermodynamic limit have the same value of X. The Anderson localization does not have this property. Close to the critical point, physi-

- cal observables are not Gaussian and generally have log-normal behavior. For discussions, see A. Aharony and A. B. Harris, Phys. Rev. Lett. **77**, 3700 – 3703 (1996); S. Wiseman and E. Domany, Phys. Rev. E **52**, 3469 – 3484 (1995), E. Orlandini, M. C. Tesi, and S. G. Whittington, J. Phys. A: Math. Gen. **35**, 4219 – 4227. (2002).
- ²⁹ A. D. Mirlin and Y. V. Fyodorov, Phys. Rev. Lett. **72**, 526 (1994).
- ³⁰ M. Janssen, Int. J. Mod. Phys. B **8**, 943 (1994).
- ³¹ K. Byczuk, W. Hofstetter, and D. Vollhardt, Phys. Rev. Lett. **94**, 056404 (2005).
- ³² D. J. Thouless, Phys. Reports **13**, 93–142 (1974).
- ³³ D. J. Thouless, J. Phys. C: Solid State Phys. **3**, 1559 (1970).
- ³⁴ M. Janssen, Phys. Rep. **295**, 1 (1998).
- ³⁵ J. Brndiar and P. Markoš, Phys. Rev. B **74**, 153103 (2006).
- ³⁶ E. Crow and K. Shimizu, eds., *Log-Normal Distribution–Theory and Applications* (Marcel Dekker, Inc., New York, 1988).
- ³⁷ *The problems encountered in early attempts to formulate cluster corrections to the DMFA are the same as those encountered in the coherent potential approximation (CPA) for disordered systems. For a detailed discussion of earlier work on the inclusion of non-local corrections to the CPA see A. Gonis, Green functions for ordered and disordered systems, in the series Studies in Mathematical Physics. Eds. E. van Groesen and E. M. DeJager (North Holland, Amsterdam, 1992).*
- ³⁸ K. Ishii, Prog. Theor. Phys. Suppl. **53**, 77 (1973).
- ³⁹ D. Vollhardt and P. Wölfle, Phys. Rev. Lett. **45**, 842 (1980).
- ⁴⁰ D. Thouless, Inter. J. Moder. Phys. B **24**, 1507 (2010).
- ⁴¹ A. MacKinnon and B. Kramer, Z. Physik B Condensed Matter **53**, 1 (1983).
- ⁴² B. Wischmann and E. Müller-Hartmann, Z. Physik B Condensed Matter **79**, 91 (1990).
- ⁴³ P. Soven, Phys. Rev. **156**, 809 (1967).
- ⁴⁴ E. Gross, E. Runge, and O. Heinonen, *Many-Particle Theory* (A. Hilger, Bristol, 1991), ISBN 9780750301558.
- ⁴⁵ A. Fetter and J. Walecka, *Quantum Theory of Many-particle Systems*, Dover books on physics (Dover Publishers Incorporated, 1971), ISBN 9780486428277.
- ⁴⁶ D. D. Johnson, Phys. Rev. B **38**, 12807 (1988).
- ⁴⁷ K. Yakubo and S. Mizutaka, J. Phys. Soc. Jpn **81**, 104707 (2012).
- ⁴⁸ P. A. Lee and D. S. Fisher, Phys. Rev. Lett. **47**, 882 (1981).
- ⁴⁹ D. H. Dunlap, K. Kundu, and P. Phillips, Phys. Rev. B **40**, 10999 (1989).
- ⁵⁰ J. A. Blackman, D. M. Esterling, and N. F. Berk, Phys. Rev. B **4**, 2412 (1971).
- ⁵¹ A. Eilmes, R. A. Römer, and M. Schreiber, Physica B: Condensed Matter **296**, 46 (2001).
- ⁵² P. Biswas, P. Cain, R. Römer, and M. Schreiber, physica status solidi (b) **218**, 205 (2000).
- ⁵³ D. Jung, G. Czycholl, and S. Kettemann, Inter. J. Moder. Phys.: Conference Series **11**, 108 (2012).
- ⁵⁴ G. Schubert, A. Weibe, G. Wellin, and H. Fehske, *HQS@HPC: Comparative numerical study of Anderson localisation in disordered electron systems in High Performance computing in Science and Engineering*, Garching 2004 (Springer, 2005).